

# Two-dimensional Time-resolved Breathing Mode Plasma Fluctuation Variation with Hall Thruster Discharge Settings

IEPC-2009-106

*Presented at the 31<sup>st</sup> International Electric Propulsion Conference,  
University of Michigan • Ann Arbor, Michigan • USA  
September 20 – 24, 2009*

Robert B. Lobbia\* and Alec D. Gallimore†

*The University of Michigan, Ann Arbor, MI, 48109, U.S.A.*

Planar measurements of near- and far-field plume-plasma fluctuations are cataloged for Hall thruster anode operation between 200 V and 400 V, with discharge currents of 1.5-A, 2-A, and 3-A. Single-point temporally resolved electron density, electron temperature, and plasma potential data are acquired by means of an electrostatic High-speed Dual Langmuir Probe (HDLP) system at 100 kHz. The observed rate of the Hall Thruster breathing mode increases from 18 kHz to 46 kHz with increasing discharge voltage at roughly 156 kHz/kV, while only 2.4 kHz/A raises are observed at larger discharge currents. Plasma oscillations from the breathing mode are strongest at the lowest anode voltage of 200 V where peak-to-peak amplitudes in excess of 90% of the mean are measured in the thruster discharge current and plasma property signals. Two-dimensional time-resolved contour maps of the plasma properties appear qualitatively similar for all operational settings, exhibiting a large burst of denser plasma emitted during each breathing mode cycle. Plasma property magnitudes quantitatively vary in approximate proportion to the discharge settings, e.g. electron density increasing by 39% in nearly direct proportion with the discharge current raising from 1.54 A to 2.06 A, and average ion transit speeds almost doubling (10.4 km/s up to 17.4 km/s) as the discharge voltage climbs from 200 V to 400 V. While these measurements represent the first detailed investigation of the breathing mode behavior within the downstream plume of a Hall thruster, they agree well with prior numerical simulation works (inclusive of dynamic effects) and, in a time-averaged manner, with independent performance measurements (where measured  $I_{sp}$  data match measured ion speed data). Permeance of large amplitude plasma oscillations into the near- and far-field plume was observed at all thruster settings suggesting the importance of the breathing mode in the discharge process. These measurements provide strong evidence for the existence of turbulent transport and increased (often labeled "anomalous" or "cross-field") electron mobility as a result of the Hall thruster breathing mode.

---

\* Ph.D. Candidate, Aerospace Engineering Dept., lobbia@umich.edu.

† Arthur F. Thurnau Professor and Laboratory Director, Aerospace Engineering Dept., alec.gallimore@umich.edu.

## I. Introduction

THE breathing mode is a low-frequency ionization instability observed in all Hall thrusters to various degrees. Typically ranging in the 10 kHz to 60 kHz band, the breathing mode has been extensively<sup>1,2,3,4</sup> investigated through examination of the transient character of the thruster discharge current signal and very-near-field single-point measurements. Quasi-time-resolved HET property measurements published by other researchers<sup>2,5,6,7</sup> show misleading trends brought about by discharge current trigger-based averaging—a technique not suitable for the chaotic nature of Hall thruster breathing mode oscillations. Recent work has dramatically extended breathing mode measurements in the near- and far-field plume (where the persistence of breathing mode fluctuations was unexpected) with planar and true real-time time-resolved (back-to-back, non-averaged) measurements presented here and elsewhere.<sup>8,9,10</sup>

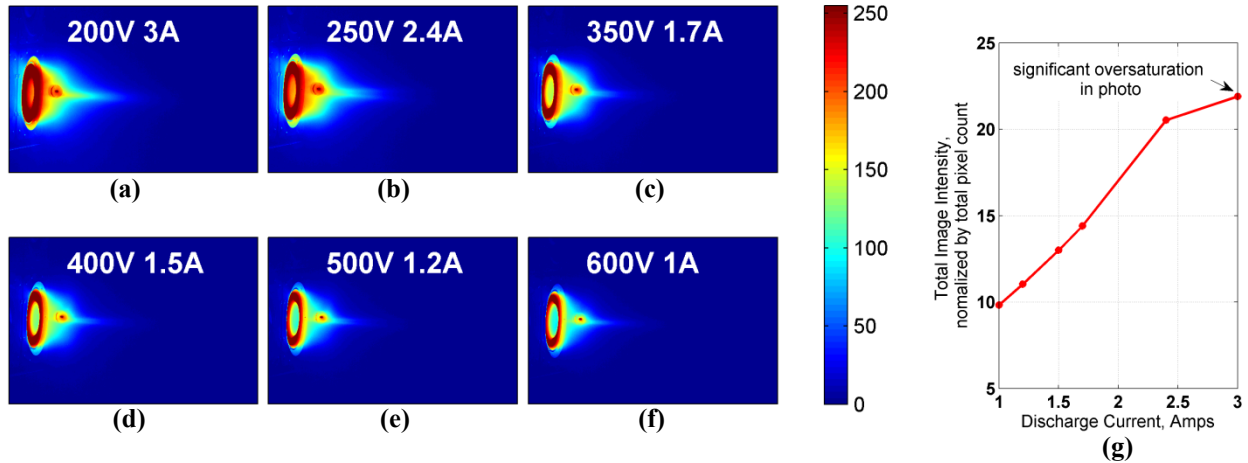


**Figure 1.** Color-mapped sequence (a)-(f) of non-filtered optical photographs taken with Nikon D80 camera using a 300 mm lens stopped down to f/13 and exposed for 1/3 s at each of the 600-W Hall thruster discharge voltage and mean discharge current settings listed. *Deceptively stable at these camera settings and to human eye, the exhausted plasma in these photos is violently oscillating at more than 15 kHz with signal peak-to-peak magnitudes nearly 90% of the DC mean. The thruster is part of a 4 engine cluster, but only single thruster operation is analyzed here. (g) shows the integrated total image intensity for each photograph, which in seen to scale roughly linearly with the mean discharge current (the highlights in the discharge channel are blown for these 8-bit images).*

## II. Experiment Overview

A specially designed High-speed Dual Langmuir (HDLP) was used to map the plume properties downstream from a 600W xenon Hall Effect Thruster (HET). The temporal resolution of plasma property measurement is set by the HDLP sweep rate which was fixed at 100 kHz using a continuous and symmetric triangle biasing waveform. Spatial resolution of 10 mm radially and 50 mm axially was selected to create a 352-element planar grid ( $R = 31$  cm by  $A = 50$  cm) that begins 10 cm downstream from the HET (thruster and side-mounted cathode centerlines are coplanar with data grid); see Figure 6(f). The two-dimensional time-resolved measurements include electron density,  $n_e(x,y,t)$ , electron temperature,  $T_e(x,y,t)$ , and plasma potential,  $V_p(x,y,t)$ . Also measured simultaneous with these properties (but sampled at 2 MHz), is the thruster discharge current (to anode),  $I_D(t)$ . All testing was performed under high-vacuum pressures (xenon-corrected ionization-gauge pressure  $< 7 \times 10^{-6}$  Torr) in the cryo-pumped 6-m by 9-m stainless-steel-clad cylindrical Large Vacuum Test Facility at the University of Michigan. The thruster magnet settings were optimized (thrust and efficiency) for cases totaling 600 W of discharged power, however for sub-600-W cases, the settings are non-optimized (and nominal magnet settings employed). More details about the HDLP system are available in prior works<sup>8,9</sup>, thus further discussion of the diagnostic is omitted in this paper.

### III. Results

As the thruster discharge voltage or the mean discharge current is increased, we find the breathing mode frequency to increase as well. In a constant 600-W power study,<sup>11</sup> the operation of the thruster followed performance trends typical to Hall thrusters (e.g. increased thrust and efficiency at higher discharge currents and voltages respectively). A great deal of HET design and tuning/optimization is based on the feedback from such traditional DC performance measurements (this includes thrust-stand, retarding potential analyzer, and all other time-averaged diagnostics). To the human eye (or a slow camera exposure as in Figure 1) most Hall thruster settings appear quite stable - which is a deceptive observation as High-speed optical imaging,<sup>5,9,10,11,12</sup> the HDLP, and other time-resolved diagnostics reveal. Indeed, it has been shown that breathing mode plasma oscillations affect thruster performance and can improve performance in certain cases.<sup>13</sup> Perhaps it should be expected that for modern high-efficiency (60% or more) Hall thrusters—all of which exhibit some degree of breathing modal behavior—that the breathing mode plays a key role in efficient thrust production.

#### A. Single-point Spectral and Temporal Thruster Plume Data

A variety of discharge settings have been studied with the 600W Hall thruster utilized in this research, and a collection of power spectral density (PSD) curves in Figure 2 displays the versatile behavior observed in the dynamics of the discharge current signal.

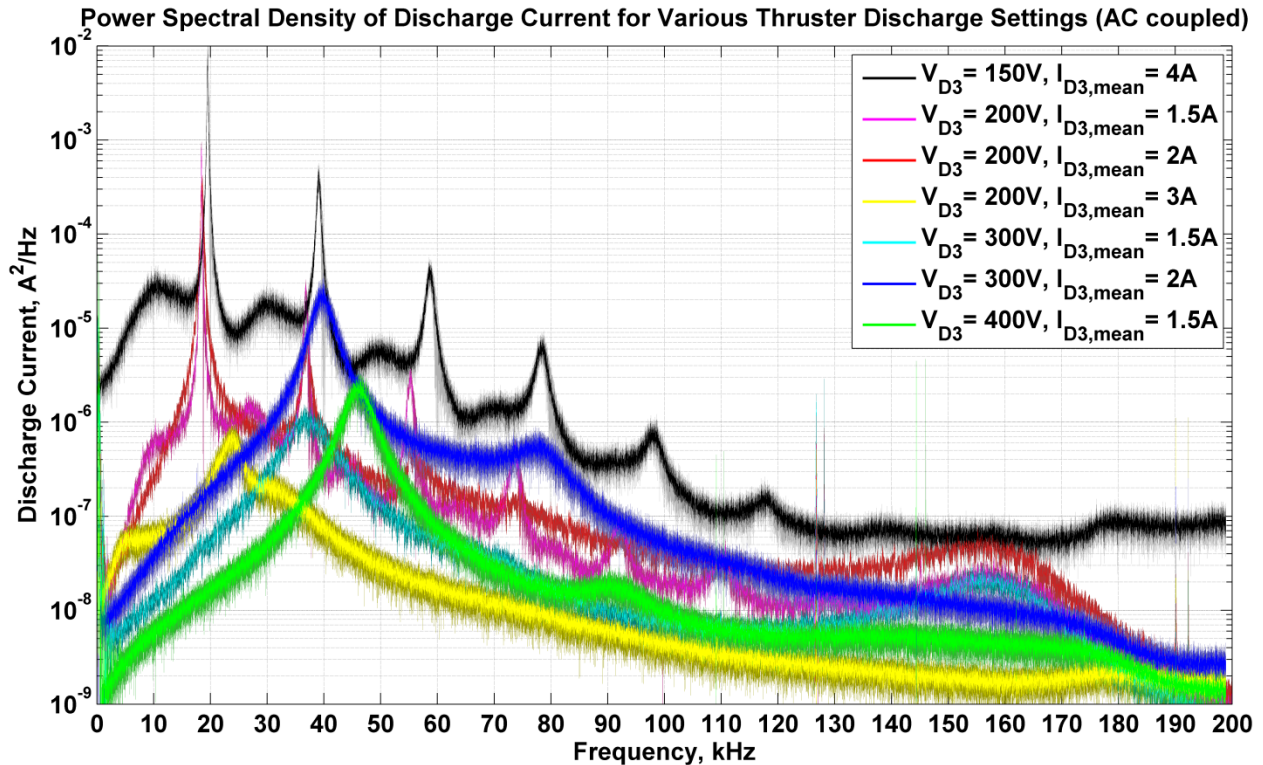


**Figure 2. Discharged current power spectral density traces (in physical  $A^2/Hz$  units) for several different discharge voltages and mean discharge currents.** *The breathing mode peak frequency dominates each operating condition with harmonics visible in most traces. The shaded region behind each spectral trace is the 95% confidence interval of the power spectral density estimates shown (each estimate uses several million samples).*

The prominent low-frequency peak observed for each setting is indicative of the thruster breathing mode,  $f_B$ ; a collection of these  $f_B$  for the thruster settings 200-V to 300-V and 1.5-A to 3-A is also available in Figure 3. For the power spectral traces, the shaded area beneath each (the 95% confidence interval) provides a measure of the statistical probability. The relatively narrow estimation envelopes suggest the thruster system possesses a stationary set of turbulent statistics for the 200 kHz bandwidth in Figure 2 for the duration of (at least) 20 seconds (the duration

of data collection). However, repeated PSD measurements on different days and with different hardware, yield indistinguishable results. One exception though is the included PSD trace for the 150-V 4-A case, where total (to date) thruster operation at this point is only around 30 minutes due to the far-from-nominal discharge current (at twice the cathode's designed current). The other cases herein presented were run for up to an hour before data collection to ensure stationary statistical behavior. In fact, it is believed that the 150-V 4-A data are experiencing a so-called "start transient,"<sup>14</sup> in which water may be outgassing from the thruster, adding additional particles to the plasma that are known to alter thruster dynamics (producing strong discharge current oscillations) in the first 10's of minutes (for post-atmospheric exposure) thruster operation.

At the lower discharge voltages (150 V and 200 V), at least 5 harmonics of the breathing mode fundamental frequency are observed in frequencies up through 100 kHz. Zooming in on the 200-V 2-A case in Figure 4, the first harmonic (37 kHz) is the second strongest feature in the measured discharge current and electron density fluctuations. Whereas, the electron temperature and plasma potential fluctuations exhibit an intermodal oscillation frequency just over 30 kHz which is of unknown origin.

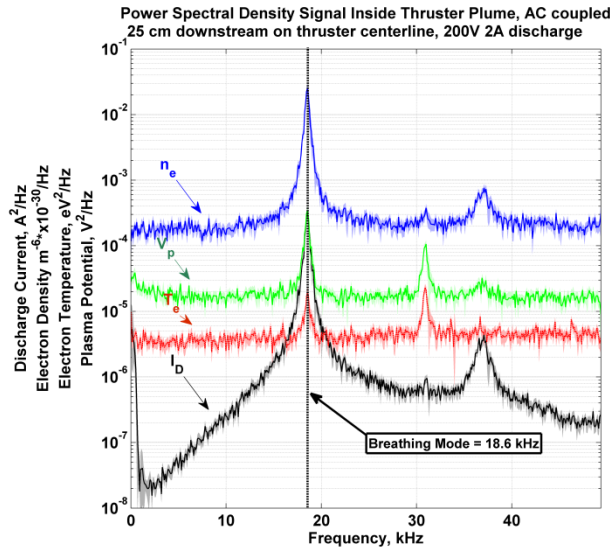


**Figure 4.** PSD for all measured signals at 25 cm downstream (on thruster centerline) of a 200V 2.0A HET discharge. Integrating total AC power using the discharge current trace yields almost 90-W of power (total power supply measured power was 420-W here).

$$f_B \approx \frac{\sqrt{U_i U_o}}{L} \approx \frac{1}{L} \left( \frac{16ek_B T_o \eta_D (V_D) V_D}{\pi m_i^2} \right)^{1/4} \quad (1)$$

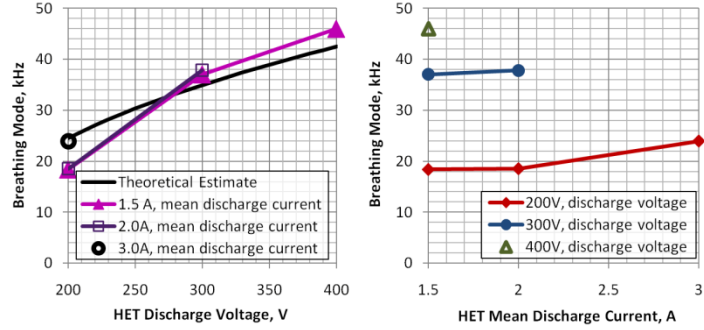


**Figure 3.** Breathing mode frequency variation with discharge voltage and mean discharge current operation of a 600-W Hall thruster. While both  $V_D$  and  $I_D$  effect the frequency of the thruster breathing mode, the discharge voltage plays a stronger role.

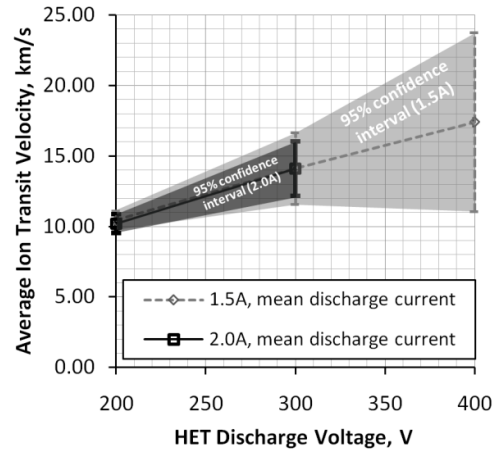


**Figure 5.** Average ion transit velocity for 200-400V operation at 1.5 and 2.0A HET discharge. The linearly expanded confidence intervals contain 95% of the collected transit delay measurements suggesting either more experimental error or more chaotic breathing mode fluctuations.

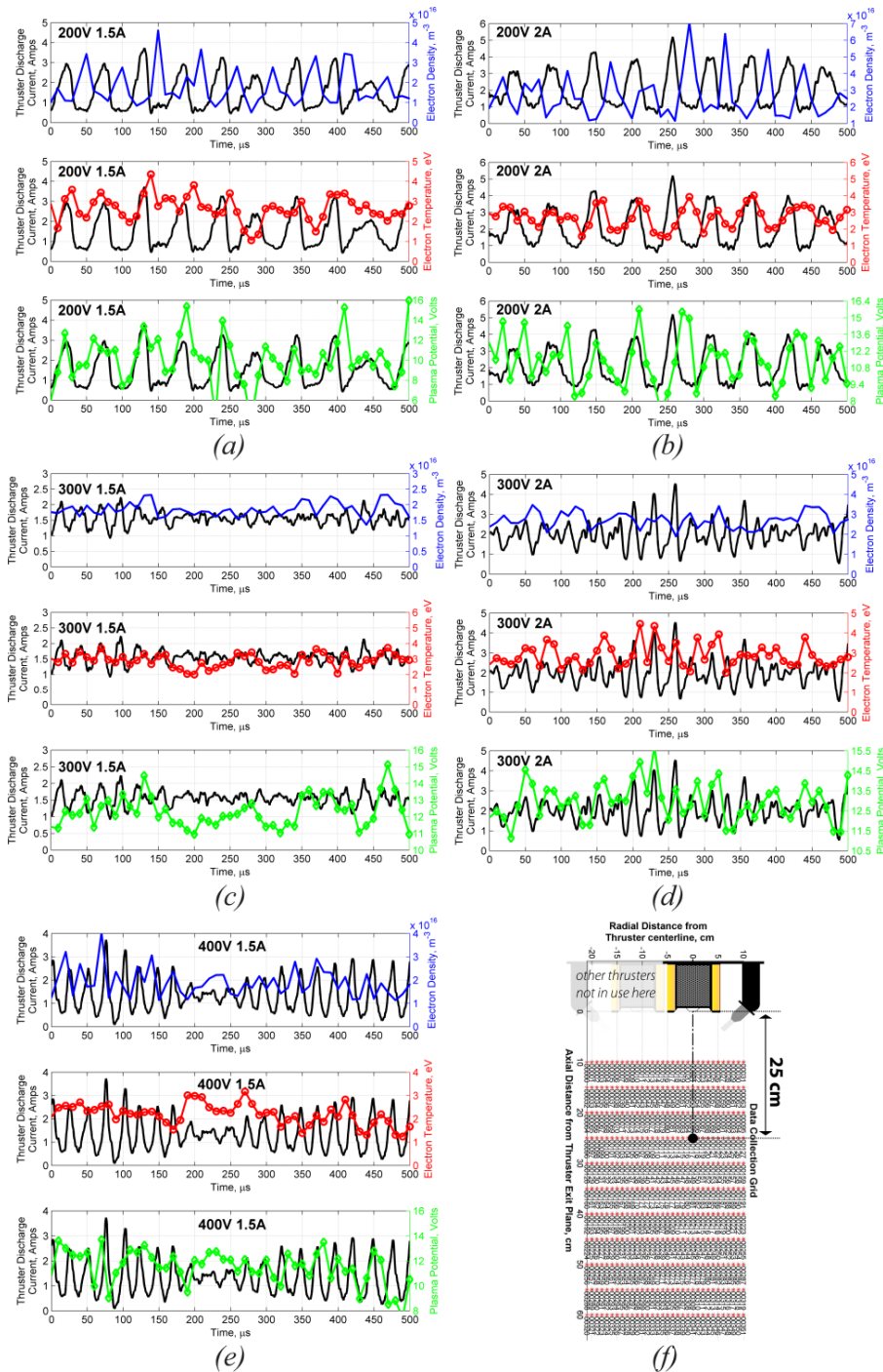


**Figure 6. Simultaneous time-resolved discharge current, electron density, electron temperature, and plasma potential, 25 cm downstream from thruster (f) shown for mean anode discharge settings: (a) 200 V and 1.5 A, (b) 200 V and 2 A, (c) 300 V and 1.5 A, (d) 300 V and 2 A, and (e) 400 V and 1.5 A. The single-point plasma properties plotted here include just 0.5 ms of the total 1 s of data gathered at each of the 352 grid-points with the 100 kHz swept HDLP diagnostic.**

In Figure 3, the breathing mode frequency variation trends with discharge voltage and mean discharge current are portrayed. The breathing mode frequency is strongly related to the discharging potential on the thruster anode as expected from simple "predator-prey" species-conservation-based breathing mode theoretical formulations such as Fife's result<sup>3</sup> that relates the  $f_B$  to the ion ( $U_i$ ) and neutral ( $U_o$ ) propellant velocities using a characteristic length scale ( $L$ , length of ionization zone) see Eq. (1).

Using room-temperature ( $T_o$  in K) thermal neutral speed, a guess at the voltage utilization efficiency function (based roughly on performance measurements<sup>11</sup>) and the mean thruster diameter as  $L$ , fair agreement with experimental data is attained. Although this simple formula gives decent results, more detailed analysis is really needed to arrive at an accurate formulation of the breathing mode frequency variation with thruster settings. For example, the magnetic field strength is known to strongly control the ionization and acceleration region positions and lengths, which is not addressed directly in Eq. (1).

The similarity of the discharge current and electron density PSD traces implies the existence of a correlation between these two signals. Physically, this is anticipated since a burst of discharge current is the result of a burst in the ionization rate. Thus birthing a large population of ions that in turn are pushed away from the

anode with the production of an impulse or thrust. These expelled ions form an ion wave, which—due to quasineutrality—gives rise to a measured increase in electron density. Taking advantage of the cross-correlation between the electron density and discharged anode current by forming a transfer function in Fourier-space, a Bode plot (not shown) is constructed. From the phase at the breathing mode frequency, a statistically accurate estimation of the ion transit-time may be computed:  $\tau_{i,t} = \frac{164.8^\circ}{360^\circ} \cdot \frac{1}{18550\text{Hz}} = 24.7\mu\text{s} \pm 1.6\mu\text{s}$ . This approach is used to generate the average ion transit velocity data shown in Figure 5. At higher discharge voltages, the increased rate of the thruster breathing mode approaches the Nyquist frequency limit (50 kHz) of the HDLP diagnostic which adds uncertainty. Additionally, the breathing mode fluctuations—while smaller in amplitude—become more chaotic and the accuracy of the correlation diminishes. These effects cause the envelope of measured average ion transit velocities to expand significantly.

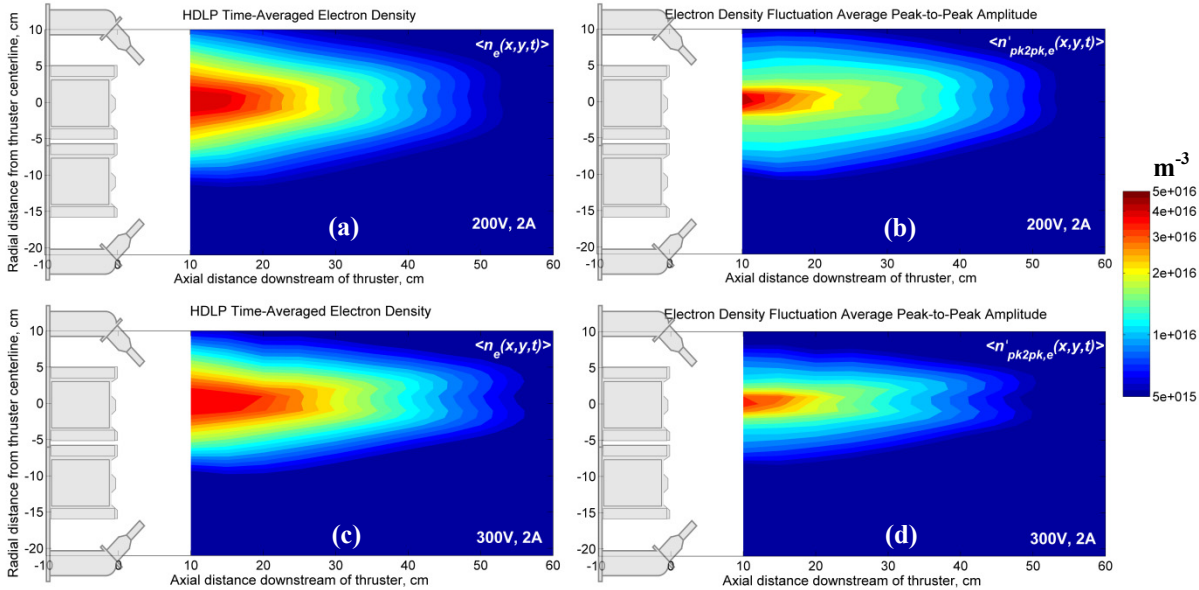


**Figure 7. Collection of planar time-averaged electron density  $\langle n_e(x,y,t) \rangle$  and fluctuation average peak-to-peak electron density amplitude  $\langle n_{e,pk2pk}(x,y,t) \rangle$ .** These averaged planar fields are computed by using all 100,000 time-resolved (with HDLP) electron density measurements obtained at each of the 352 grid points.

A series of raw HDLP time-domain data are presented in Figure 6 for the position 25 cm downstream as indicated in (f). The simultaneously measured discharge current signals are shown behind each time-resolved plasma property to in aid in visually following the thruster-plume plasma transients. The 200-V breathing mode oscillations are well defined as suggested by Figure 2 and Figure 3, with the 300-V and 400-V data revealing weaker but more chaotic wide-band oscillations. In fact, the PSD for electron temperature in Figure 3 is nearly what one would measure for a white-noise signal (e.g. a flat trace at all frequencies), but the two peaks (one at the thruster breathing mode) reveal the presence of statistically significant electron temperature oscillations within the plume. While the phase between the anode discharged current and electron density is meaningful (see Figure 5), the phase between discharge current and electron temperature or plasma potential is more complicated. Observations of raw HDLP data (as in Figure 6) imply an in-phase relation between  $I_D(t)$  and  $T_e(t)$  or  $V_p(t)$ . For plasma potential this can be explained from the nearly instantaneous propagation of electromagnetic fields (which originate in the very-near-field of the thruster and conduct through the plasma before sheaths or pre-sheaths or double-layers can even form). For electron temperature being in-phase, one only has recall the enormous thermal electron velocities and the fact that the plume region studied here is far enough away from the thruster such that the electrons are no longer magnetized. Yet, some  $T_e(t)$  and  $V_p(t)$  transients follow with phase close to that seen with the electron density. These transients are thought to be carried by the breathing mode ejected ion wave itself. The mixing of these two effects is what is believed complicate near- and far-field plume time-resolved measurements of electron temperature and plasma potential.

$V_D$ [V]	$\overline{I_D}$ [A]	$\tilde{I}_D$ [A]	$\overline{n_e}$ [ $m^{-3}$ ]	$\tilde{n}_e$ [ $m^{-3}$ ]	$\overline{T_e}$ [eV]	$\tilde{T}_e$ [eV]	$\overline{V_p}$ [V]	$\tilde{V}_p$ [V]
200	1.55	0.89	1.7E+16	9.4E+15	2.61	0.60	9.8	2.5
200	2.10	0.97	2.4E+16	9.7E+15	2.71	0.56	11.2	1.9
300	1.52	0.24	1.9E+16	3.6E+15	2.94	0.54	12.4	1.3
300	2.02	0.68	2.7E+16	6.2E+15	2.94	0.61	12.9	1.4
400	1.53	0.77	1.9E+16	6.9E+15	2.11	0.48	11.5	2.0

**Table 1. Tabulation of time-averaged and fluctuation standard deviation plasma properties 25 cm downstream (on thruster centerline) of a 600-W HET.** The " $\tilde{\quad}$ " properties are the standard deviation of the full set of time-resolved HDLP data obtained at this location. Similarly the " $\overline{\quad}$ " properties are the time-averaged values of the HDLP data.

Some statistics of the time-resolved plume plasma for the cases (a)-(e) of Figure 6 are given in Table 1. Examination of the trends in terms of the fluctuation standard deviation over mean values brings about the following intriguing result:

$$\frac{\tilde{I}_D}{I_D} \approx \frac{\tilde{n}_e}{n_e} \approx \frac{1}{2} \frac{\tilde{T}_e}{T_e} \approx \frac{1}{2} \frac{\tilde{V}_p}{V_p} \quad (2)$$

This result directly relates easily measured discharge current fluctuations to corresponding (and harder to measure) plume plasma property fluctuations. Only a single plume position is considered in Table 1, but similar ratios are observed at most plume locations measured in this study.

## B. Two-dimensional Time-resolved Thruster Plume

Figure 7 expands the result seen in Eq. (2) to the entire two-dimensional plume by comparing planar maps of the mean electron density contours to the average peak-to-peak amplitude in electron density fluctuation contours (the average peak-to-peak amplitude is used to these keep maps on an identical color-scaling, but peak-to-peak amplitude is generally proportional to standard deviation; for sinusoidal waves the proportionality is just  $2\sqrt{2}$ ). The similarity of all electron density contour maps (a), (b), (c), and (d), in Figure 7, is striking, yet since these data are all for the same mean value of 2-A discharge current, the time-averaged results are expected to be similar. The slight decrease in electron density average (peak-to-peak) fluctuation amplitude is manifested as a slight radial narrowing of the plume field. While not presented here, very similar results are seen when two Hall thrusters are operating at the same time in a clustered configuration.<sup>9</sup>

Finally, in Figure 8, a series of fully time-resolved planar density contour maps are presented for the 200-V 2-A and 300-V 2-A thruster discharge settings (for the 31-cm by 50-cm plume region at shown in prior figures). The method by which single-point HDLP time-resolved measurements are combined into two-dimensional time-resolved frames is beyond the scope of this paper and the reader is encouraged to refer to previous works that developed this unique spatial-temporal data fusion technique.<sup>8,15</sup> The left column (a) in Figure 8, includes six density frames, each separated by 10- $\mu$ s, thus portraying just over one complete breathing mode cycle (the 200-V breathing mode period is typically about 54  $\mu$ s). The right column (b) shows six equally spaced density frames for the 300-V 2-A discharge case, but since the thruster completes over two complete cycles in the 60  $\mu$ s series and since 300-V oscillations are lower in magnitude, the plasma field density oscillations appear less distinct. At the base of each column in Figure 8 the corresponding sequences of measured thruster discharge current oscillations are included with an "\*" denoting the frame series overhead. The large amplitude discharge current oscillation visible in the 200-V case (from 1-A to 4.0-A back down to 0.5-A) is typical for this thruster setting, and this very clearly generates a corresponding burst of plasma density that is ejected from the thruster at a velocity exceeding 10 km/s.

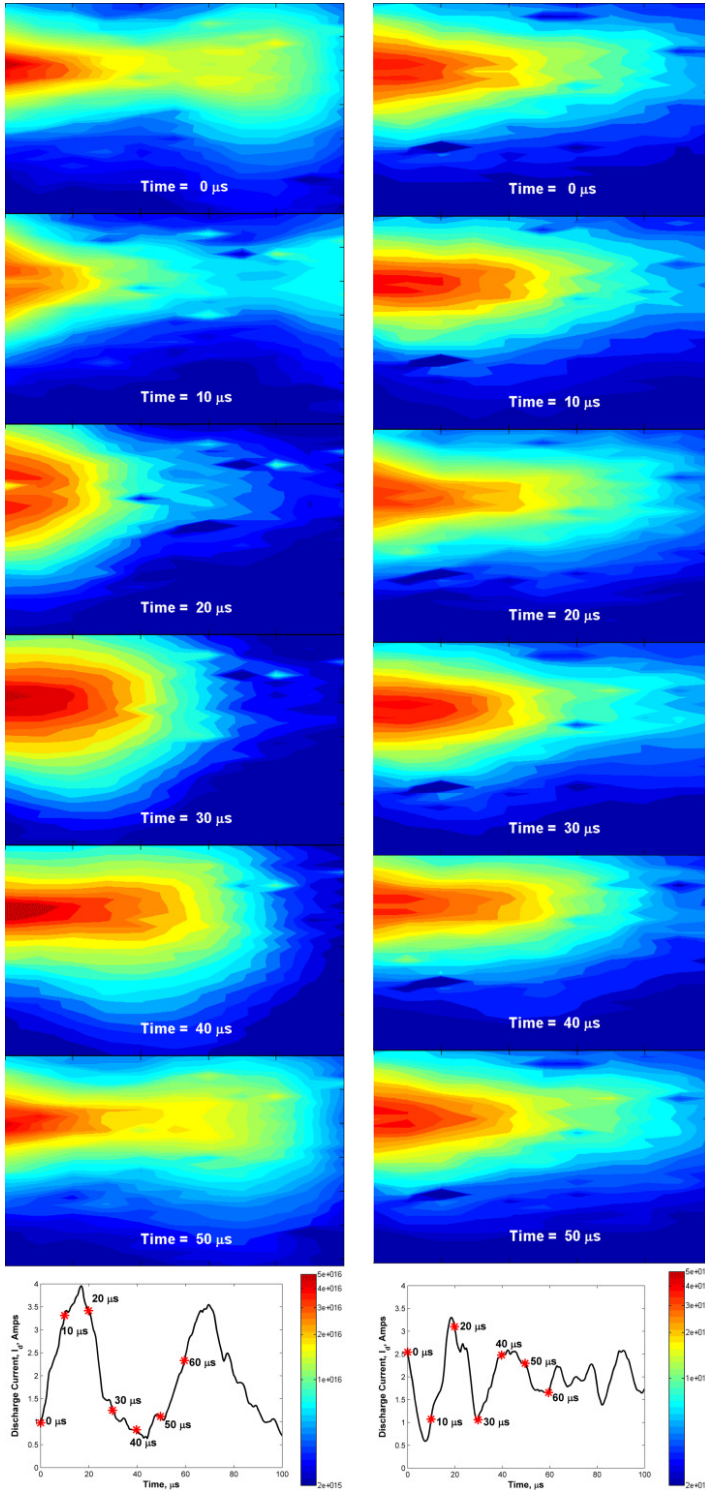


**Figure 8.** Series of time-resolved two-dimensional electron density contour maps for (a) 200 V 2 A and (b) 300 V 2 A HET discharge settings. The lower frequency of the breathing mode oscillations at 200V (18.6 kHz) provides finer temporal resolution with the 10- $\mu$ s frame-rate attained by the HDLP.

#### IV. Conclusions

In this study of time-resolved two-dimensional plasma property measurements, the influence of discharge voltage and mean discharge current were explored. The expected time-averaged trends, such as increases in discharge current producing proportional increases in electron density, were all confirmed. Theoretical breathing mode frequency estimation was also observed to follow experimental results for the predator-prey ionization instability common to all Hall thrusters. New insights on the scaling of thruster-plume fluctuations were identified, suggesting a 1:1 relationship between discharge current and electron density fluctuations. In summary, this work has shown the presence of large amplitude breathing mode oscillations at all tested thruster operating conditions. The prevalence of breathing mode oscillations (seen in the discharge current) in all Hall thrusters, at all operating conditions (but with variable amplitude), emphasizes the importance of this phenomena to the transport processes,<sup>16</sup> efficiency, and overall physics of Hall effect thruster operation.

## References

- <sup>1</sup> Choueiri, E. Y., "Plasma oscillations in Hall thrusters," *Physics of Plasmas*, vol. 8, Apr. 2001, pp. 1411-1426.
- <sup>2</sup> Bouchoule, A., Philippe-Kadlec, C., Prioul, M., Darnon, F., Lyszyk, M., Magne, L., Pagnon, D., Roche, S., Touzeau, M., and Bechu, S., "Transient phenomena in closed electron drift plasma thrusters: insights obtained in a French cooperative program," *Plasma Sources Science and Technology*, vol. 10, 2001, pp. 364-377.
- <sup>3</sup> Fife, J. M., Martinez-Sanchez, M., and Szabo, J., "A numerical study of low-frequency discharge oscillations in Hall thrusters," *33<sup>rd</sup> AIAA/ASME/SAE/ASEE Joint Propulsion Conference & Exhibit, Seattle, WA, 6-9 July 1997*.
- <sup>4</sup> Yamamoto, N., Arakawa, Y., and Komurasaki, K., "Discharge Current Oscillation in Hall Thrusters," *Journal of Propulsion and Power*, vol. 21, 2005, pp. 870-876.
- <sup>5</sup> Darnon, F., Kadlec-Philippe, C., Bouchoule, A., and Lyszyk, M., "Dynamic plasma and plume behavior of SPT thrusters," AIAA-1998-3644, *34<sup>th</sup> AIAA/ASME/SAE/ASEE Joint Propulsion Conference & Exhibit, Cleveland, OH, 1998*.
- <sup>6</sup> Pagnon, D., Roche, S., Magne, L., Touzeau, M., Bechu, S., Lasgorceix, P., Darnon, F., and Bouchoule, A., "Time resolved characterization of the plasma and the plume of a SPT thruster," AIAA-1999-2428, *35<sup>th</sup> AIAA/ASME/SAE/ASEE Joint Propulsion Conference & Exhibit, Los Angeles, CA, 1999*.
- <sup>7</sup> Albarede, L., Mazouffre, S., Bouchoule, A., and Dudeck, M., "Low-frequency electron dynamics in the near field of a Hall effect thruster," *Physics of Plasmas*, vol. 13, 2006, p. 063505.
- <sup>8</sup> Lobbia, R. B., and Gallimore, A. D., "A Method of Measuring Transient Plume Properties," AIAA-2008-4650, *44<sup>th</sup> AIAA/ASME/SAE/ASEE Joint Propulsion Conference & Exhibit, Hartford, CT, July 21-23, 2008*.
- <sup>9</sup> Lobbia, R. B., Liu, T. M., and Gallimore, A. D., "Correlating Time-Resolved Optical and Langmuir Probe Measurements of Hall Thruster Dynamics", SPS-III-36, *6<sup>th</sup> Modeling and Simulation / 4<sup>th</sup> Liquid Propulsion / 3<sup>rd</sup> Spacecraft Propulsion Joint Subcommittee JANNAF Meeting, Orlando, FL, December 8-12, 2008*.
- <sup>10</sup> Lobbia, R. B., Liu, T. M., and Gallimore, A. D., "Temporally and Spatially Resolved Measurements in the Plume of Clustered Hall Thrusters," AIAA-2009-5354, *45<sup>th</sup> AIAA/ASME/SAE/ASEE Joint Propulsion Conference & Exhibit, Denver, CO, July 2-5, 2009*.
- <sup>11</sup> Lobbia, R. B., and Gallimore, A. D., "Performance Measurements from a Cluster of Four Hall Thrusters", IEPC-2007-177, *30<sup>th</sup> International Electric Propulsion Conference, Florence, Italy, 2007*.
- <sup>12</sup> Kusamoto, D., and Komurasaki, K., "Optical Diagnosis of Plasma in a Channel of Hall Thrusters," IEPC-1997-067, *25<sup>th</sup> International Electric Propulsion Conference, Cleveland, OH, 1997*.
- <sup>13</sup> Furukawa, T., Miyasaka, T., Nakayama, E., and Soga, T., "Enhanced propulsion performances under optimum parameters in closed drift accelerators," *Vacuum*, vol. 73, 2004, pp. 407-418.
- <sup>14</sup> Hargus Jr, W., and Pote, B., "Examination of a Hall Thruster Start Transient," AIAA-2002-3956, *38<sup>th</sup> AIAA/ASME/SAE/ASEE Joint Propulsion Conference & Exhibit, Indianapolis, IN, 7-10 July, 2002*.
- <sup>15</sup> Lobbia, R. B., Gallimore, A. D., "Fusing Spatially and Temporally Separated Single-point Turbulent Plasma Flow Measurements into Two-dimensional Time-resolved Visualizations," *Presented at 12<sup>th</sup> International Conference on Information Fusion, Paper No. 243, Seattle, WA, July 6-9, 2009*.
- <sup>16</sup> Boniface, C., Garrigues, L., Hagelaar, G.J.M., Boeuf, J.P., Gawron, D., and Mazouffre, S., "Anomalous cross field electron transport in a Hall effect thruster," *Applied Physics Letters*, vol. 89, Oct. 2006, pp. 161503-3.